

A conceptual model for wind and debris impact loading of structures due to tornadoes

Baker, Christopher; Sterling, Mark

DOI:

[10.1016/j.jweia.2017.11.029](https://doi.org/10.1016/j.jweia.2017.11.029)

License:

Creative Commons: Attribution-NonCommercial-NoDerivs (CC BY-NC-ND)

Document Version

Peer reviewed version

Citation for published version (Harvard):

Baker, C & Sterling, M 2018, 'A conceptual model for wind and debris impact loading of structures due to tornadoes', *Journal of Wind Engineering and Industrial Aerodynamics*, vol. 175, pp. 283-291.
<https://doi.org/10.1016/j.jweia.2017.11.029>

[Link to publication on Research at Birmingham portal](#)

General rights

Unless a licence is specified above, all rights (including copyright and moral rights) in this document are retained by the authors and/or the copyright holders. The express permission of the copyright holder must be obtained for any use of this material other than for purposes permitted by law.

- Users may freely distribute the URL that is used to identify this publication.
- Users may download and/or print one copy of the publication from the University of Birmingham research portal for the purpose of private study or non-commercial research.
- User may use extracts from the document in line with the concept of 'fair dealing' under the Copyright, Designs and Patents Act 1988 (?)
- Users may not further distribute the material nor use it for the purposes of commercial gain.

Where a licence is displayed above, please note the terms and conditions of the licence govern your use of this document.

When citing, please reference the published version.

Take down policy

While the University of Birmingham exercises care and attention in making items available there are rare occasions when an item has been uploaded in error or has been deemed to be commercially or otherwise sensitive.

If you believe that this is the case for this document, please contact UBIRA@lists.bham.ac.uk providing details and we will remove access to the work immediately and investigate.

C J Baker*, M Sterling

School of Engineering, University of Birmingham

Edgbaston, Birmingham, B15 2TT, United Kingdom

* Corresponding author c.j.baker@bham.ac.uk

Abstract

This paper presents a novel conceptual design framework which takes into account the direct wind loads and pressure loads acting on a structure due to the passing of a tornado. Furthermore, for the first time, the potential damage due to debris impact has been incorporated enabling a holistic assessment of structural loading to be considered. The model is built on a recently developed wind and pressure field model that captures the main features of tornadoes, which is used to generate a large number of tornado wind and pressure field realisations from which values of particular load effects can be determined. A cumulative distribution function of load effect is thus derived, which can be combined with tornado climatology probabilities to determine load effects at a particular risk level. This use of this framework is illustrated through two examples – the direct wind and pressure loads on a low-rise portal frame structure, and the debris loads on a medium rise rectangular structure.

Keywords – tornado, wind loads, debris impact, design framework

1. Introduction

Since wind engineering was first defined as a discipline in the 1960s, most attention has been focussed on the effects of large-scale windstorms on structures – particularly tropical and extra-tropical cyclones. This has resulted in a robust set of wind engineering tools for design, encapsulated in codified design methods for a wide variety of structures using the results of extensive wind tunnel and full scale testing, within a conceptual framework first developed by Davenport and the other early pioneers of wind engineering (Davenport 1982). In recent years however it has come to be realised that the effects of smaller, transient wind storms can be of significance – frontal gusts, thunderstorm downbursts and tornadoes in particular – and there is significant ongoing research in this area. Much of this work has been focussed on full-scale observations of such wind systems (eg Bluestein et al 2003, Orwig et al 2007, Duranona et al 2006) and physical and numerical modelling (eg Haan et al, 2008, Mishra 2008a, b, Case et al, 2013, Jesson et al 2015a, b). Only very recently have methodologies begun to emerge to incorporate these transient wind effects into the design process - see De Gaetano et al (2014) and Solari (2014) for a discussion of loading due to thunderstorm downbursts, and Kareem et al (2016) for a more general structure to incorporate transient effects into design, which reduces to the Davenport methodology for statistically stationary wind events. Design for such transient winds usually requires a time series approach, as the traditional spectral based methods make the assumption that the wind loading is statistically stationary. In a review by Letchford (2015), the wide range of issues that arise from codification of non-synoptic winds are discussed and a framework is proposed based on the “design response spectrum” methodology used in earthquake engineering. This

utilises a range of real earthquake time histories applied to a range of structures of different natural frequencies to specify displacements, velocities and accelerations that can be used for design purposes. The major problem of applying either this method or time history based methods for downbursts and tornadoes is the lack of full-scale wind velocity and pressure time histories, particularly with regard to tornadoes.

This paper is specifically concerned with the wind loads due to tornadoes. Now, tornadoes are widely classified using the Fujita or enhanced Fujita scales (Fujita, 1991, WERC 2006) which allocates tornadoes to one of five categories. This essentially classifies tornadoes by the damage they cause and thus effectively integrates both the wind loading and the building vulnerability, and inevitably the range of wind speeds associated with any one Fujita classification is large. Whilst a useful descriptor, this classification does not actually specify the parameters required for a wind loading design. Now, the wind loading due to tornadoes is particularly complex and consists of a number of components. Firstly we have what might be termed direct wind loads – loads caused by the variable surface pressures on the structures due to the local velocities, in a similar manner to the loads caused by synoptic winds, although it can be expected that these loads will be transitory in terms of time, magnitude and direction, and cannot be regarded as stationary. Also, close to the core of the tornado, the vertical component of the wind speed may be of significance and effect these surface pressures. Secondly there will be loads caused by the differences between the low atmospheric pressure in the core of the tornado, and the non-equalised internal pressure within the structure. The magnitude of the latter will be dependent on the nature of the envelope porosity and the presence, or otherwise, of any dominant opening,

and again can be expected to be highly transitory. Finally, within tornadoes there can be expected to be significant impact loads from flying debris from either natural sources (trees, soil and gravel etc.) or from damaged buildings (roof and wall components etc.). Such debris can be observed in tornadoes and effectively visualise the tornado funnel cloud (Noda, 2014).

Tornado loading is usually taken into account only for highly sensitive structures such as nuclear power plants. The methodology used in the US nuclear industry is given in USNRC (2007). There, a design wind speed is given which has a probability of occurrence of 10^{-7} for each of three regions of the USA, and the pressure loads are then calculated from the application of a very simple Rankine vortex model. Debris impact velocities are also given for a small range of debris types (pipes, automobiles and metal spheres), taken from a numerical solution of trajectories, using a different wind field model developed by Simiu and Scanlon (1996). However, a conceptual method of how all these essentially time varying loading effects could be incorporated into design for a range of risk levels is yet to be developed, although there is some ongoing work by Tamura et al (2015) that is attempting to build a tornado database for use in design in Japan. It is nonetheless clear that a pre-requisite of such a method is a consistent and simple description of the tornado flow field that could be used in design to predict velocity and pressure time histories and to enable debris trajectories to be calculated. Further, to enable such a formulation to be used to generate the large number of cases needed for either a time history method or the design response spectrum method described above, requires that it be relatively simple and quick to apply (i.e. not a complex numerical calculation). Such a wind field / debris trajectory model has recently been developed by the authors and is reported in Baker (2016).

Section 2 summarises the main points of this wind and debris trajectory model. We then build on this to develop a consistent risk based approach to tornado wind loading due to the three mechanisms described above. Section 3 considers the wind and pressure fields in translating tornadoes and section 4 sets out a conceptual framework for the tornado wind load design process. The calculation of direct wind loads and pressure loads is then described and illustrated in section 5, and the calculation of debris impact loads in tornadoes is set out and similarly illustrated in section 6. The model is discussed and concluding remarks made in section 7.

2. The tornado wind field and debris trajectory model

The model outlined in Baker (2016) starts by assuming the following expression for the radial velocity of a single celled tornado vortex.

$$\bar{U} = \frac{-4\bar{r}\bar{z}}{(1+\bar{r}^2)(1+\bar{z}^2)} \quad (1)$$

where $\bar{U} = U/U_m$; U and U_m are the radial velocity and maximum radial velocity respectively; $\bar{r} = r/r_m$; r and r_m are the radial distance from the centre of the vortex and a radial length scale respectively; $\bar{z} = z/z_m$; z and z_m are the vertical distance from the centre of the vortex and vertical length scale respectively. This expression thus gives a peak in the radial inflow velocity in both the radial and vertical directions and thus seems physically plausible. It effectively aims to model the tornado ground boundary layer, through forcing a velocity reduction close to the ground. By substituting this expression into the continuity equation and the circumferential and radial momentum equations one obtains the following

expressions for the normalised circumferential velocity $\bar{V} = V/U_m$ and normalised pressure $\bar{P} = p/\rho u_m^2$

$$\bar{V} = \frac{2.88S\bar{r}[\ln(1+\bar{z}^2)]}{(1+\bar{r}^2)} \quad (2)$$

$$\bar{P} = -\frac{8\bar{r}^2\bar{z}}{(1+\bar{r}^2)^2(1+\bar{z}^2)^2} - \frac{4.15S^2(\ln(1+\bar{z}^2))^2}{(1+\bar{r}^2)} - \frac{4\ln(1+\bar{z}^2)(1-\bar{z}^2)}{(1+\bar{r}^2)^2(1+\bar{z}^2)^2} \quad (3)$$

where V is the circumferential velocity, p is the pressure, ρ is the density of the flow and S is the swirl ratio, the ratio of the maximum circumferential velocity to the maximum radial velocity.

$$S = \frac{V_M}{U_M} \quad (4)$$

Expressions can also be derived for the vertical velocity and buoyancy force but are not considered here. In this paper we will define the parameters that will be used in the loading as the velocities and pressures at the edge of the boundary layer i.e., $\bar{z} = 1$. This results in the rather simpler expressions which will be used in what follows.

$$\bar{U} = \frac{-2\bar{r}}{(1+\bar{r}^2)} \quad (5)$$

$$\bar{V} = \frac{2S\bar{r}}{(1+\bar{r}^2)} \quad (6)$$

$$\bar{P} = -\frac{2\bar{r}^2}{(1+\bar{r}^2)^2} - \frac{2S^2}{(1+\bar{r}^2)} \quad (7)$$

Using the debris theory developed by Baker (2007), the debris trajectory analysis was carried out for compact debris only i.e. for debris where the aerodynamic forces are characterised by a drag coefficient (C_D) only, on the basis that such a formulation is appropriate for the large time behaviour of both compact and sheet debris. The analysis revealed that the trajectory is dependent upon the swirl ratio S , the initial debris trajectory positions \bar{r}_o and \bar{z}_o and two further parameters given by

$$\Phi = \frac{0.5\rho A r_m}{M} C_D \quad \Psi = \frac{g r_m}{u_m^2} \quad (8)$$

where A is the debris area, M is the debris mass, and C_D is the debris drag coefficient. the first group in equation (8) is the buoyancy parameter, whilst the second is an inverse tornado Froude number. The Tachikawa number, which is normally used to characterise debris flight (Holmes et al (2006)) is given by the ratio Φ/Ψ . In broad terms, the debris trajectories are much more dependent upon S and Φ than on \bar{r}_o, \bar{z}_o and Ψ - for example whether or not debris flies or falls in a tornado is largely a function of its position in the S / Φ plane. This will be seen to be of significance in what follows.

3. Tornado translation

To be able to use the above vortex model in any design methodology, we need to allow for vortex translation in some way. To do this we make the following assumptions.

- The structure under consideration is at $(0, \bar{Y})$, where $\bar{Y} = Y/r_m$ and Y being the lateral distance from the tornado track centre line;
- The tornado moves at a dimensionless speed $\bar{Q} = Q/U_m$ along the x axis, where Q is the dimensional speed, and passes through the origin at a normalized time $\bar{t} = t r_m / U_m = 0$ (t represents the actual time);
- The total dimensionless wind speed \bar{V} at the structure, is the vector sum of tornado wind speeds and tornado translational speed \bar{Q} ;
- All velocities and pressures are defined at $\bar{z}=1$ i.e. the top of the tornado ground boundary layer.

This is represented graphically in figure 1. Note however that the model tests of Fleming et al (2013) suggest that a simple superposition of the translation velocity on the vortex velocity field is not totally adequate, and that translation may result in the vortex tilting with height. Nonetheless, these assumptions result in the following expressions for \bar{V} and ϕ , the latter being the observed wind direction relative to the x -axis.

$$\bar{V} = \left(\left(\bar{Q} + \bar{U} \frac{\bar{X}}{(\bar{X}^2 + \bar{Y}^2)^{0.5}} - \bar{V} \frac{\bar{Y}}{(\bar{X}^2 + \bar{Y}^2)^{0.5}} \right)^2 + \left(\bar{U} \frac{\bar{Y}}{(\bar{X}^2 + \bar{Y}^2)^{0.5}} + \bar{V} \frac{\bar{X}}{(\bar{X}^2 + \bar{Y}^2)^{0.5}} \right)^2 \right)^{0.5} \quad (9)$$

$$\phi = \tan^{-1} \left(\frac{\bar{U} \frac{\bar{Y}}{(\bar{X}^2 + \bar{Y}^2)^{0.5}} + \bar{V} \frac{\bar{X}}{(\bar{X}^2 + \bar{Y}^2)^{0.5}}}{\bar{Q} + \bar{U} \frac{\bar{X}}{(\bar{X}^2 + \bar{Y}^2)^{0.5}} - \bar{V} \frac{\bar{Y}}{(\bar{X}^2 + \bar{Y}^2)^{0.5}}} \right) \quad (10)$$

where $\bar{X} = \bar{Q}\bar{t}$. The dimensionless velocities \bar{U} and \bar{V} are the radial and circumferential tornado velocities from equations (5) and (6), with $\bar{r}^2 = \bar{X}^2 + \bar{Y}^2$. Similarly the pressure time history can be found from equation (7) with \bar{r} so defined and $\bar{z} = 1$, i.e. at the top of the boundary layer.

Figure 2 below shows a brief parametric analysis about a standard case for which $\bar{Y} = 0.5$, $S=1$, $\bar{Q} = 0.5$. The value of translational velocity is rather higher than would be expected in reality, but the choice of such a value allows a large variation in the parametric analysis that in turn enables a clear variation in the calculated velocities to be seen. The left hand figures show the magnitude of velocity at the building position, and the right hand figures show polar plots of the magnitude of observed wind speed against wind direction. Note the complexity and large variability of the former and the relative simplicity of the latter with the velocity variation given by elliptical shape. In particular it can be seen that the effect of changing \bar{Y} is to change the size and shape of ellipse; the effect of changing S is to twist the ellipse; and the effect of changing \bar{Q} is to translate the ellipse..

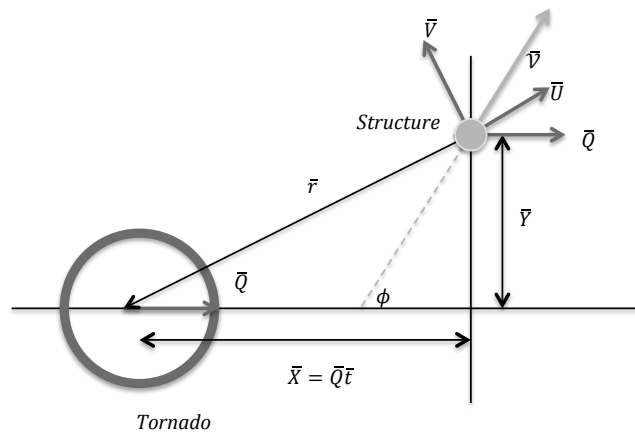
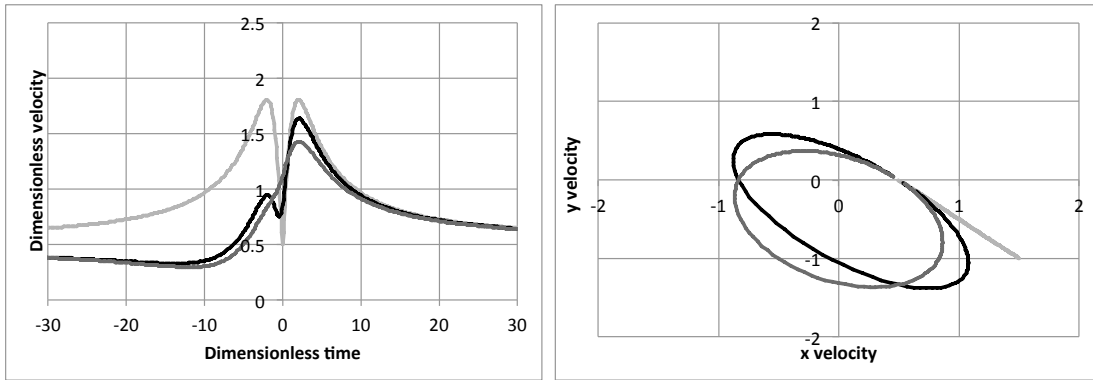
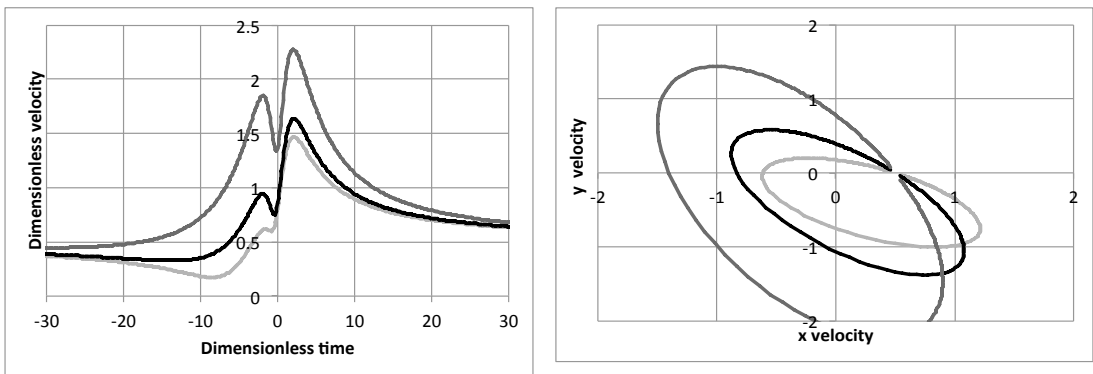


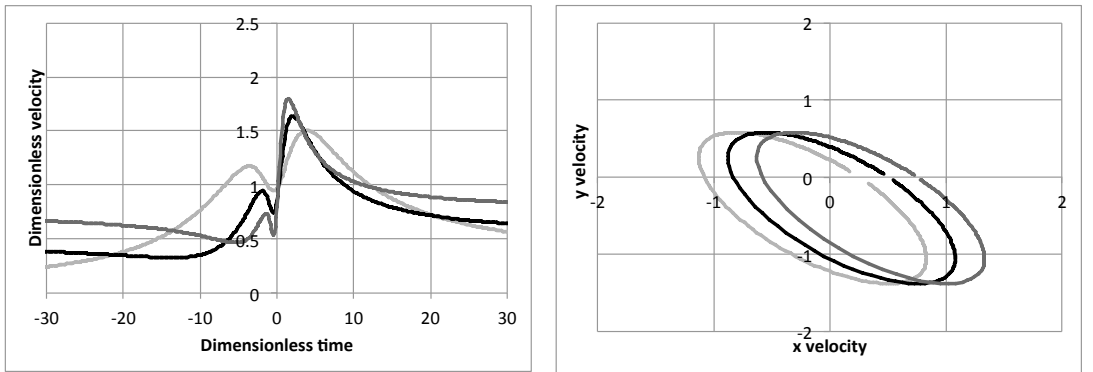
Figure 1 Tornado translation - open circle shows tornado travelling along x axis; small closed circle shows structure under considerations



Light grey $\bar{Y} = 0$, Black $\bar{Y} = 0.5$, Dark grey $\bar{Y} = 1$



Light grey $S = 0$, Black $S = 0.5$, Dark grey $S = 1$



Light grey $\bar{Q} = 0.25$, Black $\bar{Q} = 0.5$, Dark grey $\bar{Q} = 0.75$

(a) Magnitudes relative to observer

(b) Polar plot of magnitude and direction

Figure 2 Parametric analysis of winds at structure position around $\bar{Y} = 0.5, S=1, \bar{Q} = 0.5$

4. Conceptual loading design framework

In this section we consider the outline of the conceptual model that is the main subject of this paper. Firstly, however it is worth considering what would be an appropriate level of complexity in the determination of tornado wind effects for design. Perhaps the major characteristics of tornadoes are their complexity and their variability and the capture of all the necessary characteristics by a simple model is probably unrealistic. This has led some authors to consider the complex nature of tornadoes using large scale numerical simulations – see Lin et al (2015) for example. Now whilst such approaches undoubtedly capture much of the complexity of tornadoes, they do so for a very particular set of input parameters, and thus cannot represent the variability. The high level of resource required by such simulations implies that they cannot be used many times to capture the variability between tornado events. Thus the basic principle that is followed in this work is the use of a simple tornado model that captures the basic characteristics of such events, and can be used multiple times to understand the variability of tornado loadings for very many cases. In other words the model seeks to capture tornado variability, albeit with the loss of detail and the simplification of complexities.

The conceptual model that we adopt in this paper has two related components – one to find the load due to time varying tornado wind velocities and pressures, and one to find the debris impact loading. The output from both components is the same – cumulative distribution functions of loads for different probabilities of occurrence. Consider first the direct wind load / pressure load model schematic in figure 3a. This may be considered to consist of an outer model and an inner model. The outer model requires the following inputs.

- Structural properties – building type and geometry, dynamic characteristics if appropriate.
- Characteristics of tornadoes at the site in question – pdfs of maximum speed, swirl ratio, radius, translational speed etc.
- Tornado climate data in the form of number of tornados (above a certain threshold in strength) per square kilometre per year.

The outer model then generates a large number (usually 1000) of tornado realisations based on the input probability density function and for random variations of distance from the structure and angle to the main axis of the structure, which are then used by the inner model (see below) to generate realisations of the specific load effect under consideration. A cumulative distribution function of load effects is thus generated, that is convoluted with the tornado climate probabilities to find a relationship between the magnitude of the load effect and its related probability (purple box).

The inner model generates the tornado velocity and pressure time histories, and uses these to calculate specific load effects. The direct wind load component calculates the velocity time history relative to the stationary building and then uses surface pressure data from physical model (tornado vortex generator) or CFD calculations, as a function of wind direction, to calculate the quasi-steady wind loads. Corrections for lack of velocity correlation over the structure and for dynamic effects can then be applied to give inertial load time histories (using weighting functions and dynamic multipliers), The pressure load component (green boxes) calculates the pressure load time history for one set of input variables, and also calculates the internal pressure within the structure using a suitable internal pressure model that allows for envelope leakage and, if present,

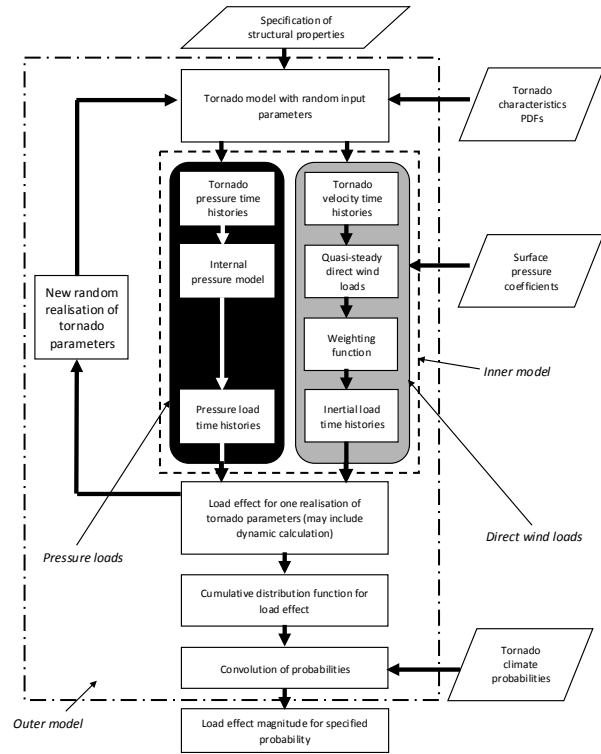
a dominant opening the latter also requiring velocity time history information. The difference between the internal and external pressure then gives a pressure load on the cladding on the structure. The inertial and pressure load component are then combined within a load effect calculation (which may be either a static or a dynamic calculation) to give one load effect realisation.

The debris impact model (figure 3b) is similar in form, but does not adopt a time history approach. For each realisation of tornado parameters, a cumulative distribution function of debris impact loads on the structure for that realisation is obtained from pre-calculated debris trajectories. Thus a multi-realisation cumulative distribution function (CDF) for debris impact loads can be calculated, through a large number of tornado realisations which can again be convoluted with the probability of a tornado actually occurring to give a relationship between the magnitude of a specific impact and its probability of occurring. Taken together the two models can be used to predict wind loads and debris impact loads at consistent probability levels.

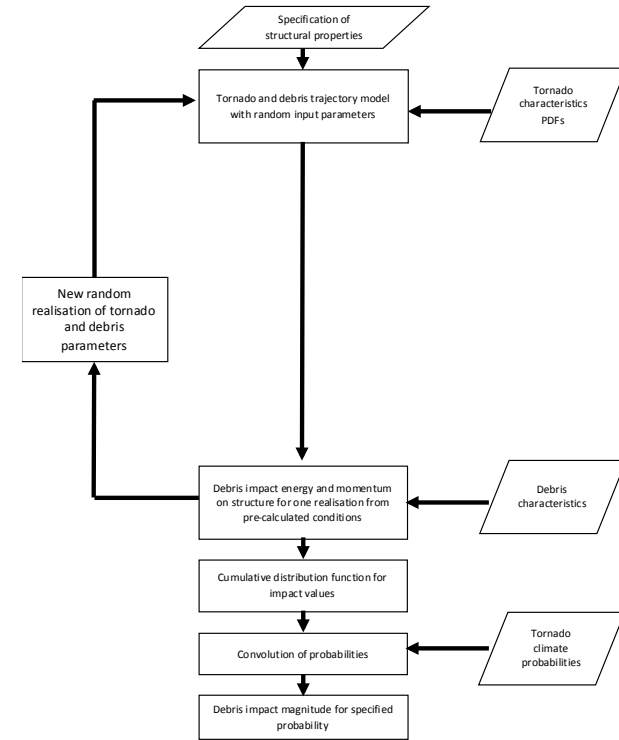
In what follows we give more detail of the individual components of this model and illustrate its use with examples. We do not consider further however the tornado climatology, i.e. the probability of tornadoes actually occurring. Datasets that allow tornado probabilities to be determined in any one location are beginning to emerge (see Kirk (2014) for the UK situation for example, Ramsdell (2007) for the USA and Tamura et al (2015) for emerging statistics from Japan), and some probabilistic information on tornado strength and size is also becoming available - again see Tamura et al (2015). However, as in so many aspects of the model presented here, further full scale data is required in this area. The paper of Tamura et al also proposes an outline for a design methodology for tornado wind

and pressure loads, and a simple flow chart is presented. It appears however it is based on a deterministic set of tornado and debris parameters, rather than the statistical approach presented here.

1



(a) Inertial and pressure loads



(b) Debris loads

Figure 3 The conceptual model

2

3 **5. Calculation of inertial and pressure loads**

4 **5.1 Direct wind loads**

5 The calculation of direct wind loads is through the use of wind speeds and
6 pressure coefficients in a manner that is similar to the calculation for boundary
7 layer winds. The wind speed time histories (magnitude \bar{R} and direction ϕ) can be
8 calculated from the methodology of section 3. The pressure coefficients ideally
9 need to be determined from Tornado Vortex Generator measurements (for
10 different building distances from the vortex core (\bar{Y}) and wind directions), or from
11 equivalent CFD calculations, and thus to properly allow for the highly curved flow
12 in tornadoes, with significant vertical velocity components. Experiments of this
13 type are reported by Mishra (2008) and Case et al (2013). The surface pressure
14 on the structure ($P_e(t)$) is then related to the velocity and pressure coefficient
15 ($C_p(\phi)$) by the equation

$$16 \quad P_e(t) - P_r(t) = 0.5\rho\bar{R}(t)^2 C_p(\phi) \quad (11)$$

17 Here $P_r(\bar{t})$ is the local reference pressure – effectively the time varying pressure at
18 the building position. This is effectively a quasi-steady assumption, and assumes
19 the instantaneous pressure can be directly related to an instantaneous velocity,
20 through a measured pressure coefficient. These pressure coefficients can then be
21 suitably summed to obtain a load effect such as overall drag or lift forces. However,
22 if the structure is of any size then these pressures will not be correlated over the
23 full extent of the structure, and some method needs to be used to allow for this
24 non-correlation. A possible way forward is to use the weighting function approach
25 adopted by Sterling et al (2009) for flow around trains (the time domain
26 equivalent of the frequency spectrum) that would then filter out the high
27 frequency fluctuations. Also the rapidly changing flow velocity and direction

28 could in principle lead to dynamic overshoots, which can in principle be calculated
29 using a method such as that of Mason (2016), which was derived from the well
30 known Morrison equation.

31 The problem with such an approach is that there is, at present, a shortage of
32 suitable pressure coefficient data obtained with sufficient spatial and directional
33 resolution, and almost no information on weighting functions or dynamic
34 correction factors, and compromises must be made in what data is used if
35 calculations are to be carried out. As an illustration of such a calculation, let us
36 consider the case of the tornado wind uplift on the roof of a structure with a plan
37 area of 10m x 5m with a 30 degree roof pitch. The pressure coefficients are taken
38 from the directional method of BS6399 (BSI (1997)) and are thus strictly only for
39 boundary layer winds, but do allow a directional variation to be determined. The
40 variation of overall lift force coefficient (C_L) with wind direction from using this
41 data is shown in figure 4. The lift coefficient force here is given by

$$42 \quad C_L = \frac{L}{0.5\rho A_R R^2} \quad (12)$$

43 where L is the overall lift, A_R is the roof area and R is the dimensional resultant
44 wind speed. Note that the lift force here is defined in terms of a local velocity. A
45 quasi-steady approach is then followed and no weighting function or dynamic
46 correction is applied. Figure 5 shows a small number of typical time histories of
47 lift force due to inertial or wind effects. In this figure the lift force coefficient
48 definition is based on the tornado reference wind speed, i.e.

$$49 \quad C_{LW} = \frac{L}{0.5\rho A_R U_m^2} \quad (13)$$

50 The immediate point to note is that these time histories are very variable in form
51 and magnitude, as indeed one would expect because of the significant variation in

52 tornado parameters, building distance from the core etc. Unsurprisingly the large
 53 loads occur when the vortex core passes near the structure, and for when the
 54 tornado swirl values are high.

55

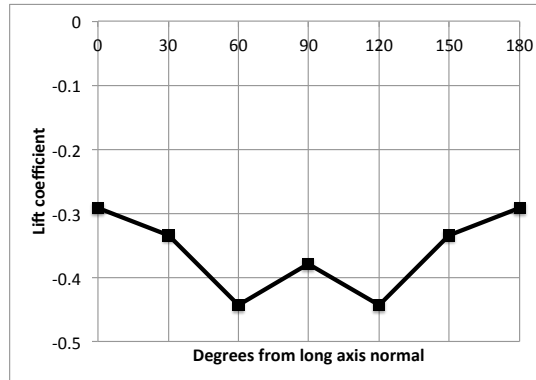
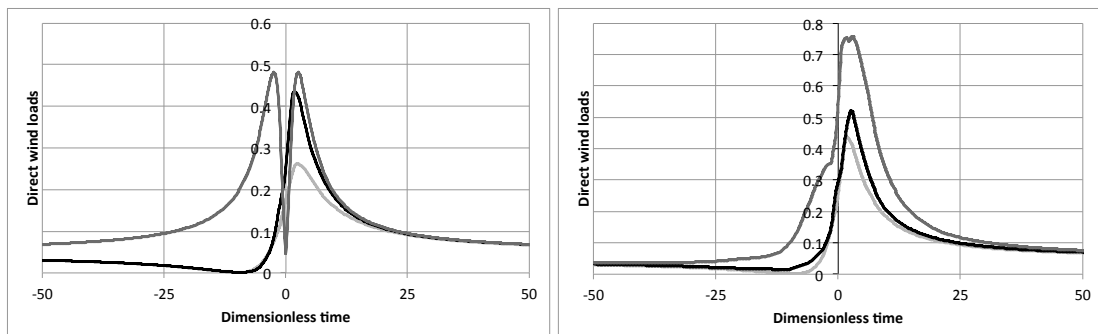


Figure 4 Pitched roof lift coefficients from BS6399 Directional Method

56



(a) Variation with \bar{Y} ($\bar{Q}=0.4$; $S=1$; light grey $\bar{Y} = 2$, black $\bar{Y} = 1$, dark grey $\bar{Y} = 0$)

(b) Variation with S ($\bar{Q} = 0.4$; $\bar{Y} = 1$; light grey $S = 1$, black $S = 2$, dark grey $S = 4$)

4)

Figure 5 Direct wind load variation – lift coefficient C_{LW}

57 5.2 Pressure loads

58 The pressure loads on a structure are caused by the pressure differential between
 59 the outside and the inside of the building. As the low pressure in the centre of a
 60 tornado passes over the building, then, if the building is well sealed with small
 61 leakage, then the internal pressure will remain high and only decrease slowly. This

62 can result in a significant pressure differential across the building envelope and
63 thus large cladding forces. If there is a significant dominant opening in the
64 building, then the pressure at the opening will be given by the instantaneous
65 pressure coefficient at that point, and may result in significant acoustic pressure
66 oscillations (eg Ginger et al, 2008). In the current methodology, the pressure time
67 history is given by equation (6) in a moving frame of reference, and the internal
68 pressure can be calculated from a suitable unsteady internal pressure analysis,
69 such as those set out in Guha et al (2011) or Levitz et al (2013). For the leakage
70 only case, the method of Guha et al gives the equation.

$$71 \quad \Pi \frac{dC_{pi}}{d\bar{t}} = \text{sgn}(C_{pe} - C_{pi}) \sqrt{|C_{pe} - C_{pi}|} \quad (14)$$

72 where $C_{pi} = \frac{P - P_a}{0.5\rho U_m^2}$ is the internal pressure coefficient; $C_{pe} = \frac{P - P_a}{0.5\rho U_m^2} = 2\bar{P}$ is the
73 tornado induced pressure coefficient, and P_a is a reference pressure measured
74 outside the tornado. The parameter Π is given by

$$75 \quad \Pi = (0.5\rho U_m^2 V_s) / (C_d \gamma P_a A_s r_m) \quad (15)$$

76 where V_s and A_s are the volume and leakage area of the structure, C_d is the leakage
77 discharge coefficient (taken as 0.6 in what follows) and γ is the ratio of specific
78 heats. The value of Π thus varies with the tornado and building properties. The
79 overall lift force due to pressure effects is then given by

$$80 \quad C_{LP} = C_{pi} - C_{pe} \quad (16)$$

81 Taking further the example building in the last section, we assume a volume of
82 500m³ (and thus a height to the eaves of 9.3m) and a leakage area of 0.1m². Figure
83 6 shows a typical time history of internal and external pressures for a structure
84 beneath the vortex core. The lag of the internal and external pressure variations
85 can be clearly seen.

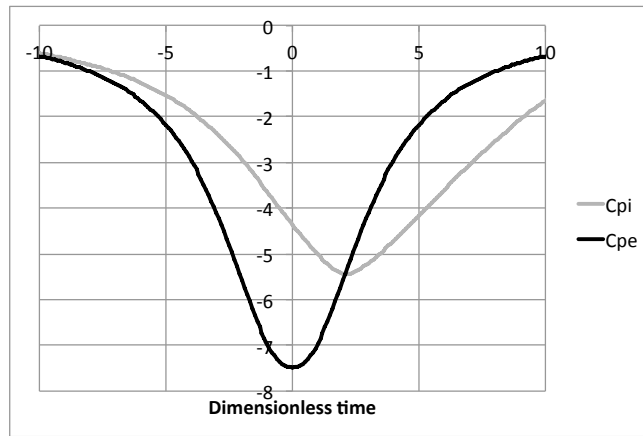
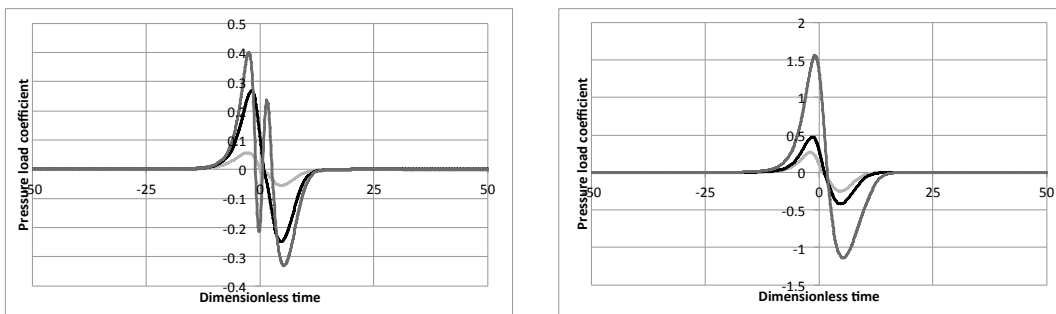


Figure 6 External and internal pressure variation ($\bar{Q}=0.4; S=4; \bar{Y} = 0; \Pi = 0.5$)

87 Typical pressure load time histories (for the same cases as in figure 5) are shown
 88 in figure 7. As for the direct wind loads, the time histories are very variable, both
 89 in form and in magnitude, with the large values occurring for buildings close to
 90 the tornado track, at high swirl ratios.



(a) Variation with \bar{Y} ($\bar{Q}=0.4; S=1$; light grey $\bar{Y} = 2$, black $\bar{Y} = 1$, dark grey $\bar{Y} = 0$)

(b) Variation with S ($\bar{Q} = 0.4; \bar{Y} = 1$; light grey $S = 1$, black $S = 2$, dark grey $S = 3$)

4)

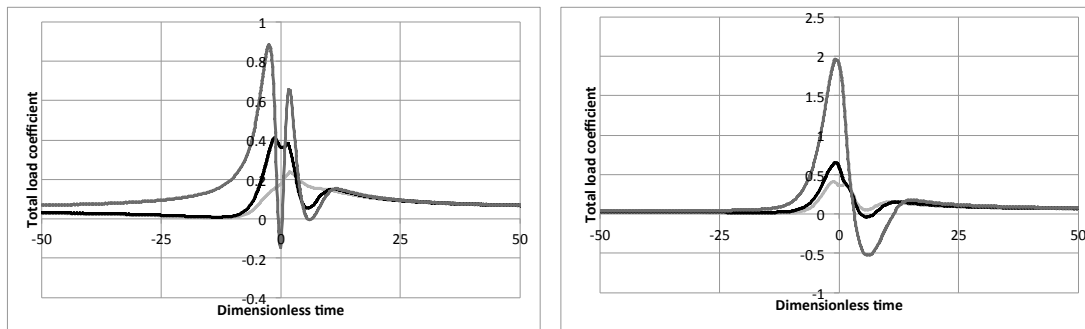
Figure 7 Pressure load variation C_{LP}

91

92

93 **5.3 Total loads**

94 The total loads can be obtained by summing the inertial and pressure loads. Again
 95 typical time histories are shown in figure 8. The form of these time histories can
 96 again be seen to be complex, and for some the direct wind loads dominate, and for
 97 others the pressure loads dominate.
 98



(a) Variation with \bar{Y} ($\bar{Q}=0.4$; $S=1$; light grey $\bar{Y} = 2$, black $\bar{Y} = 1$, dark grey $\bar{Y} = 0$)

(b) Variation with S ($\bar{Q} = 0.4$; $\bar{Y} = 1$; light grey $S = 1$, black $S = 2$, dark grey $S =$

4)

Figure 8 Total load variation – the sum of C_{LW} and C_{LP}

99 In order to incorporate the above analysis into a probabilistic framework, a
 100 thousand realisations of tornado characteristics were calculated for the tornado
 101 parameters shown in table 1, and the maximum roof lift for the building calculated
 102 in every case. These parameters represent a medium strength tornado passing
 103 within 500m of the structure. The values for the assumed characteristics seem
 104 reasonable, but can only be regarded as approximations to reality. Note that no
 105 interaction between the different tornado parameters is assumed here. The data
 106 given in Tamura et al (2015) from early US work and work in Japan, suggests a
 107 weak interaction between core radius and maximum wind speed, and a rather
 108 stronger interdependence between translational speed and maximum wind
 109 speed. Such interactions can in principle be allowed for, but in view of the

110 uncertainties involved, this aspect is not taken further in this paper. Figure 9
 111 shows the cumulative distribution function of the dimensional load values. These
 112 effectively show the cumulative probability distribution that the tornado induced
 113 lift on the structure will exceed a certain value. To obtain a design probability,
 114 these values must be multiplied by the probability that the tornado will be within
 115 500m of the structure, data for which needs to come from tornado climate
 116 probabilities. Note that for the situation under consideration (a 5m x 10m pitched
 117 roof building) the design lift for synoptic winds could be expected to be in the
 118 order of 10 to 15 kN, around the 70th percentile of tornado loading for the assumed
 119 tornado characteristics.

120

Table 1 Tornado parameters

Parameter	V_m (m/s)	U_m (m/s)	Q (m/s)	r_m (m)	Y_0 (m)	Building angle
Distribution	Normal	Normal	Normal	Normal	Uniform	Uniform
Mean	40	20	10	100	0 to	0 to 90°
SD	10	2	2	20	500m	

121

122

123

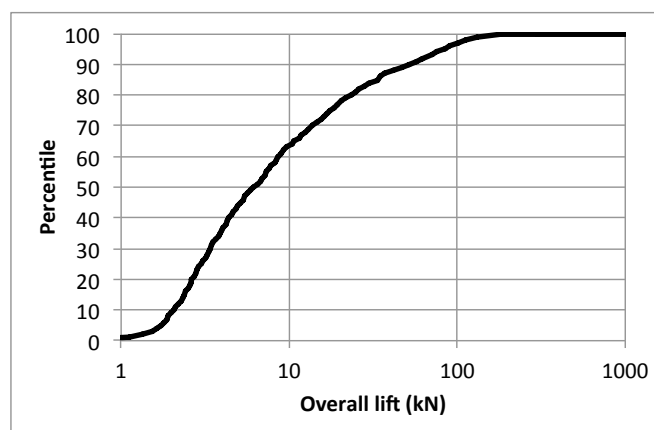


**Figure 9 Cumulative distribution function for tornado wind loading for
assumed parameter set**

124

125

126 **6. Debris loads**

127 The procedure for calculating tornado debris impact loads is somewhat different
128 from that for direct wind loads. Whilst a large number (1000) of tornado
129 simulations are still carried out, the maximum impact loads for each realisation
130 are carried out using pre-calculated tables and the maximum values for each
131 realisation are then used to give the overall CDF for impact loading. Now, in terms
132 of debris impact, the two most commonly used parameters to specify the impact
133 are the debris kinetic energy and momentum. In what follows we concentrate on
134 the former, although the same analysis could be applied to the latter. In
135 dimensionless terms the potential debris impact energy on a structure can be
136 expressed in the functional form:

137
$$\bar{E} = \frac{0.5M(U^2+V^2)}{\rho A r_m U_m^2 C_D} = \frac{0.5(\bar{U}^2+\bar{V}^2)}{\Phi} = fn(S, \Phi, \Psi, \bar{Y}, \bar{H}, \bar{r}_0, \bar{z}_0) \quad (17)$$

138 where \bar{Y} is the closest dimensionless distance of the building from the tornado
139 centre and \bar{H} is the dimensionless building height. \bar{r}_0 and \bar{z}_0 are the initial debris
140 positions. In terms of impact on structures, the important parameter is the
141 maximum value of the dimensionless energy \bar{E}_{max} when the debris is within the
142 range $\bar{r} > \bar{Y}$ and $\bar{z} < \bar{H}$, i.e. within the cross section of the tornado flow field
143 where debris might impact upon the building as the tornado passed by. There is
144 an implicit assumption here that the building size is small in relation to the
145 tornado size. This is not wholly adequate and any future development of the

146 methodology will need to address this issue. In preliminary studies it was found
147 that, as expected, the values of \bar{E}_{max} were insensitive to debris starting position,
148 as long as this was reasonably close to the vortex centre, and also insensitive to
149 changes in the parameter Ψ . This is in line with the observations on the sensitivity
150 of debris trajectories made in section 2. This allows a considerable simplification,
151 and the above functional expression becomes:

$$152 \quad \bar{E}_{max} = fn(S, \Phi, \bar{Y}, \bar{H}) \quad (18)$$

153 Debris trajectory simulations to calculate \bar{E}_{max} were thus carried out for a wide
154 range of values of S , Φ , Ψ , \bar{Y} and \bar{H} , and a series of “look up” tables created. For
155 these simulations the stationary tornado model was used. For each of the
156 thousand realisations of tornado parameters in the framework of figure 3b, a
157 hundred realisations of debris parameters were simulated, based on probability
158 distributions of debris mass and area (which give a pdf for Φ). For each debris
159 realisation, the value of \bar{E}_{max} was found, and thus the maximum value for all
160 debris flight realisations for each tornado parameter realisation was found. From
161 the thousand tornado realisations the overall CDF of debris impact loads could
162 thus be found. Figure 10 shows the results of such a calculation for a 40m high,
163 10m square building, passed by a tornado with the statistical tornado parameters
164 taken from table 1. The statistical values for the debris parameters are shown in
165 table 2, these values being representative of those observed in recent small scale
166 tornadoes in the UK. The debris statistics can of course be changed to suit
167 particular geographical circumstances. This approach effectively assumes there is
168 a source of debris for each realisation close to the centre of the vortex – in physical
169 terms this might be from a failing building for example. This gives the debris
170 impact energy CDF in the same form as the overall wind loading CDF of figure 9,

171 and it is thus possible to design a structure for a balanced probability of direct
172 wind / pressure loading and debris impact loading.

173

Table 2 Debris parameters

Parameter	$M (kg)$	$A(m^2)$
Distribution	Normal	Normal
Mean	0.2	0.1
SD	0.05	0.02

174

175

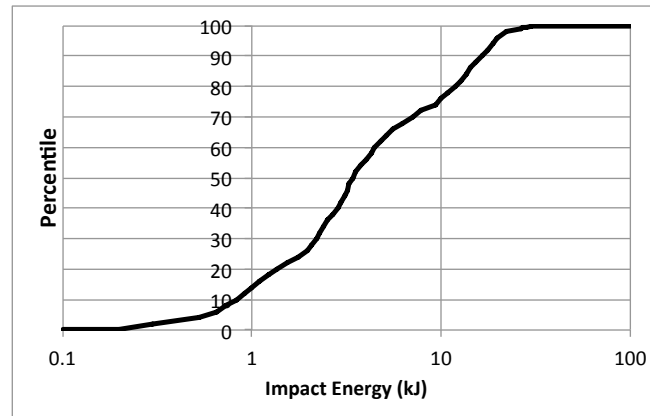


Figure 10 Cumulative distribution function for debris impact

176

177

178

179 **7. Discussion and concluding remarks**

180 In this paper we have set out simple analytical models for the velocity and
181 pressure fields in tornado vortex and for the calculation of debris trajectories in
182 such a vortex, and then used this model as the core component of a conceptual
183 model for wind and debris impact loading in tornadoes. The novel developments
184 in this modelling approach are as follows.

185 • The conceptual model of tornado loading that has been developed allows
186 wind loading (inertial loading and pressure loading) to be calculated for a
187 large number of tornado realisations, using the above model, and thus
188 allows the CDF of tornado loading to be derived, which, through
189 convolution with tornado climate data, will enable design loadings to be
190 determined.

191 • Similarly the methodology allows debris impact loading CDFs to be
192 determined in a consistent way with the wind loading, allowing for loading
193 probabilities for both wind and impact loading to be aligned.

194 These points being noted however, there is still work to be done before the
195 conceptual framework can be used routinely in design, both in terms of model
196 development and in terms of required data.

197 • The tornado model (outlined in Baker (2016)) is weak in its treatment of
198 the tornado boundary layer and tornado turbulence, and development is
199 required here – although more full-scale experiments are required to
200 inform and validate such developments. Similarly, the model is for one-cell
201 tornado vortices only, whereas in reality two-cell vortices are common.
202 Baker (2016) presents a possible methodology for deriving a two-cell
203 vortex model, but again this requires development and validation.

204 • The debris trajectory model is at the moment only developed for compact
205 debris. Whilst this may also be a fair representation for the long-term
206 trajectories of small sheet debris where the major aerodynamic force as it
207 approaches its asymptotic speed is the aerodynamic drag, the same is
208 probably not true for large sheet debris, where the velocity field may vary

209 across the width of the debris and is certainly not the case for rod debris.

210 Further development is needed here.

211 • The method of allowing for vortex translation may not fully capture
212 dynamic translational effects.

213 • The conceptual model for wind loading (inertial and pressure loads) needs
214 information on tornado statistical parameters (mean and standard
215 deviation of velocities, size etc). More information is needed here to give
216 confidence in the values that were assumed.

217 • The direct wind-loading model requires structural force coefficients that
218 have been obtained in physical or numerical simulations of tornadoes.
219 Obtaining such information is a major task that will require significant
220 resource.

221 • The pressure-loading model needs to be developed further to include the
222 modelling of dominant openings.

223 • To date, the wind loading methodology has only been applied to static
224 structures, and a dynamic methodology of appropriate complexity needs
225 to be added (i.e. one that can be used in a large number of simulations with
226 computational efficiency).

227 • The debris impact model requires as input debris statistical parameters.
228 Discussion is required within the engineering community as to what
229 parameters are appropriate for different types of structural design.

230 Again, these points being made, the conceptual model presented in this paper has
231 the potential for providing a useful tool for use in structural design in the future,
232 as further full scale and model scale information becomes available.

233

234 **References**

- 235 Baker C J 2016, Debris flight in tornadoes, 8th Conference on Bluff Body
236 Aerodynamics and its Applications, Boston, USA
- 237 BSI (1997) Loadings for Buildings – Part 2 Code of Practice for Wind Loads. British
238 Standard 6399 Part 2 (withdrawn).
- 239 Bluestein H, Lee W-C, Bell M, Weiss C, Pazmany A (2003) Mobile Doppler Radar
240 Observations of a Tornado in a Supercell near Bassett, Nebraska, on 5 June 1999.
241 Part II: Tornado-Vortex Structure, Monthly Weather Review 131, 2968-2984
- 242 Case J, Sarkar P, Sritharan S (2013) Effect of low-rise building geometry on
243 tornado-induced loads, 12th Americas Conference on Wind Engineering Seattle,
244 USA
- 245 Davenport A G (1982) The interaction of wind and structures, Engineering
246 Meteorology 1527-572
- 247 De Gaetano P, Repetto M P, Repetto T, Solari G (2014) Separation and classification
248 of extreme wind events from anemometric records, Journal of Wind Engineering
249 and Industrial Aerodynamics 126, 132-143
- 250 Durañona V, Sterling M, Baker C J (2006) An analysis of extreme non-synoptic
251 winds, Journal of Wind Engineering and Industrial Aerodynamics 95, 1007-1027
- 252 Fleming M R, Haan F L, Partha P, Sarkar P (2013) Turbulent Structure of Tornado
253 Boundary Layers with Translation and Surface Roughness, 12th Americas
254 Conference on Wind Engineering Seattle, USA
- 255 Fujita T (1991) Proposed Characterization of Tornadoes and Hurricanes by Area
256 and Intensity, SMRP Research Paper No. 91, University of Illinois
- 257 Ginger J D, Holmes J D, Kopp G A, (2008) Effect of building volume and opening
258 size on fluctuating internal pressure, Wind and Structures 11, 361–376.

259 Guha T K, Sharma R N, Richards P J (2011) Internal pressure dynamics of a leaky
260 building with a dominant opening, Journal of Wind Engineering and Industrial
261 Aerodynamics 99, 1151-1161

262 Haan F L, Sarkar P P, Gallus W A (2008) Design, construction and performance of
263 a large tornado simulator for wind engineering applications, Engineering
264 Structures 30, 1146-1159

265 Holmes J D, Baker C J, Tamura Y (2006) Tachikawa number: A proposal, Journal of
266 Wind Engineering and Industrial Aerodynamics, 94, 1, 41-47

267 Jesson M, Sterling M, Letchford C W, Baker C J (2015a) Aerodynamic Forces on the
268 roofs of low-mid- and high-rise buildings subject to transient winds, Journal of
269 Wind Engineering and Industrial Aerodynamics 143, 42-49

270 Jesson, M., Sterling, M., Letchford, C and Haines M (2015b) Aerodynamic forces on
271 generic buildings subject to transient downburst-type winds. Journal of Wind
272 Engineering and Industrial Aerodynamics. 137, 58-68

273 Kareem A, Gao Y, Hu L (2016) Time-frequency domain modelling framework for
274 non- stationary aerodynamic load effects, 8th Conference on Bluff Body
275 Aerodynamics and its Applications, Boston, USA

276 Kirk P J (2014) An updated tornado climatology for the UK: 1981-2010, Weather,
277 69, 7, 171-175, 10.1002/wea.2247

278 Letchford C, Lombardo F (2015) Is codification of non-synoptic wind loads
279 possible?, 14th International Conference on Wind Engineering, Brazil

280 Levitz B, Letchford C, James D (2013) Dynamics of Internal Pressures During
281 Tornado Events, 12th Americas Conference on Wind Engineering Seattle, USA

282 Lin W E, Savory E, Ozyoruk A N, Orf L G (2015) Analysis of an EF5 tornado
283 embedded within a simulated supercell windstorm, 14th International Conference
284 on Wind Engineering, Brazil

285 Mason M, Yang T, 2016 Unsteady pressures on a square cylinder subjected to
286 transient wind fields, UK Wind Engineering Society Conference, Nottingham

287 Mishra A R, James D L, Letchford C W (2008a) Physical simulation of a single-
288 celled tornado-like vortex, Part A: flow field characterization, Journal of Wind
289 Engineering and Industrial Aerodynamics 96, 1258–1273

290 Mishra A R, James D L, Letchford C W (2008b) Physical simulation of a single-
291 celled tornado-like vortex, Part B: wind loading on a cubical model, Journal of
292 Wind Engineering and Industrial Aerodynamics 96, 1258–1273

293 Orwig K D, Schroeder J L (2007) Near surface wind characteristics of extreme
294 thunderstorm outflows, Journal of Wind Engineering and Industrial
295 Aerodynamics 95, 565-584

296 Ramsdell, J V (2007), "Tornado Climatology of the Contiguous United States, Rev
297 2, NUREG/CR-4461 Prepared for U.S. Nuclear Regulatory Commission, 2007

298 Simiu E, Scanlan R (1996) Wind Effects on Structures: Fundamentals and
299 Applications to Design, 3rd Edition, John Wiley & Sons, Hoboken, NJ

300 Solari G (2014) Emerging issues and new frameworks for wind loading on
301 structures in mixed climates., Wind and Structures 19, 3, 295-320.

302 Sterling M, Baker C, Bouferrouk A, O'Neil H, Wood S, Crosbie E (2009) An
303 investigation of the aerodynamic admittances and aerodynamic weighting
304 functions of trains, Journal of Wind Engineering and Industrial Aerodynamics 97,
305 512-522

306 Tamura Y, Matsui M, Kawana S, Kobayashi F (2015) Statistical properties of

307 tornadoes in Japan and tornado risk model for nuclear power plants, 14th
308 International Conference on Wind Engineering, Brazil
309 USNRC (2007) Design basis tornados and tornado missiles for nuclear power
310 plants, US Nuclear Regulatory Commission
311 WERC (2006) A recommendation for an enhanced Fujita scale, Wind Engineering
312 Research Centre, Texas Tech University, [http://www.spc.noaa.gov/efscale/ef-](http://www.spc.noaa.gov/efscale/ef-ttu.pdf)
313 [ttu.pdf](http://www.spc.noaa.gov/efscale/ef-ttu.pdf)

314

315 **Funding**

316 This research did not receive any specific grant from funding agencies in the
317 public, commercial, or not-for-profit sectors.

318